ELSEVIER

PII: S0141-0296(97)00072-2

Engineering Structures, Vol. 20, No. 3, pp. 134–143, 1998

0141-0296/98 $19.00 + 0.00

Design of an active mass damper for a tall TV tower in Nanjing, China

H. Cao, A. M. Reinhorn and T. T. Soong

Department of Civil Engineering, State University of New York at Buffalo, Buffalo, NY 14260, USA

The design of an active mass damper to reduce the effects of wind vibrations on a tall (340 m) communication tower in Nanjing, China is presented herein. The existing tower has excessive vibrations under the design wind loads, beyond the comfort level. The design of a mass damper needs to meet several constraints resulting from space, strength and power limitations. The selection of an active alternative for the mass damper is the result of economical and performance considerations within the specified constraints. The paper emphasizes the use of a single mode approach for the design evaluations vs the multi-modal approach. Nonlinear control strategies combined with the design constraints produce a feasible solution for the damper design. The paper emphasizes the system approach to the design in which the performance, the physical constraints and the implementation issues, such as power–force relations and frictional effects, are simultaneously considered. Neglecting any of the above issues may result in an inadequate solution. © 1997 Elsevier Science Ltd.

Keywords: mass damper, active control, wind forces, earthquake

1. Introduction

The response induced by wind-storms has a severe influence on tall structures such as high-rises and tall towers. Such wind-storms may be considered in the structural design while the necessary strength is provided to the structure. However, the control of vibrations and the performance for extreme events may require a substantial increase in the construction costs. Special performance provisions regarding the comfort of occupants during such extreme vents are practically non-existent. For such cases, a control system, either passive or active can be cost-effective in assuring continuous occupancy and service.

Passive and active control systems, such as mass dampers or bracing systems were suggested, investigated and constructed in the US, Japan and elsewhere, during the last two decades[1–3]. All the active control implementations in building structures were made by Japanese industries in the last decade[2,3]. The principle of the active systems is to provide external corrective forces in strategic points in the structure to constrain the response within predetermined performance limits[4]. Active bracing systems[5,6] and active variable stiffness systems[3] are systems built of conventional structural components of structures enhanced with external forces that modify either the effective damping, or the natural frequency of the system to produce more efficient vibration suppression. However, use of such systems requires an intervention or modification of the structural system, usually prohibitive in existing large structures.

Mass dampers are additional large weights added to the structure[4] or isolated from the main structural system[7], which can absorb, through their large movement, energy transferred from the main structure. Their action is similar to increasing the damping in the main structure, therefore, the name 'mass dampers'. The advantage of such a system is that it does not require major intrusion in the structural system, therefore, is suitable for retrofit cases. The addition of an active force to the mass damper[8] can improve the efficiency by increasing the operation frequency range and by limiting some of the excessive movement of the mass itself. Implementations of such mass systems in high-rise structures, in the form of special added masses, or water/ice containers already used for other services in the building[2], or in the form of a heliport platform[7], were made recently in Japan.

Therefore, due to the flexibility in locating the damper and the least intrusion in the structural system, a mass damper was selected to control the excessive vibrations of

the Nanjing TV tower during extreme wind-storms. However, the design of such a mass damping system requires a simultaneous consideration of performance objectives and constraints imposed by the existing construction, by the available resources and by the cost-efficiency.

2. Structural design considerations

The existing tower (~340 m) made of a reinforced concrete core with three large supporting piers, has two observation decks (at 200 and 240 m elevations). A steel antenna extends above the upper observation deck to the top of the tower (see *Figure 1*). During wind storms the vibrations of the observation deck are beyond the comfort limit of 15 mg ($= 0.15$ m/s^2) set as performance criterion. The suggested solutions for vibration reduction is to add a mass damper to improve the comfort during severe storms, which are characterized by a mean wind speed of 20.7 m/s at 10 m elevation assuming a 50-year return period.

The design of such a mass damper had to meet several constraints, due to the fact that the structure is already constructed and most available spaces are in use, or are planned for future service. Therefore, the design of the damper had to meet special restrictions:

(a) No floor space in the observation deck was found available. Therefore, the system needs to be suspended. Pendulum type systems, hanged as mass rings outside the tower[4] cannot be used, due to architectural and service constraints (exterior communication wires and conducts). Interior suspended pendulum rings[4,9] cannot be constructed, since there is not enough head room.

(b) The interior floor in the observation deck has a limited load capacity which limits the additional mass and the additional supporting structure to less than 80 tons.

(c) The access for construction crews and materials is limited to elevators that carry less than 0.9 ton (~1.7 Kips). Moreover, the narrow access doors and transport spaces require on-site assembly of any system, practically made of components.

(d) Mass dampers usually are constructed with a spring-recentering system tuned to the structural frequencies. Mechanical springs, or pendulum type, were used in similar applications[3], but are costly and require space for implementation. Gas (nitrogen) springs are used in other applications[10]. However, such springs become nonlinear at large pressures generated from large stroke.

(e) The implementation of any damper needs to meet (i) the realistic conditions of friction in mechanical parts, or in the supporting structure, (ii) the large movements imposing extremely large strokes in actuators, and (iii) sustained power action for long periods of time during wind storms.

In the following sections the design of the active mass damper is described, starting with the functional requirements and progressing with the solutions for various constraints.

3. Active control strategy

The wind effect in the tower will be reduced by using an active mass damper designed using a general control sche-

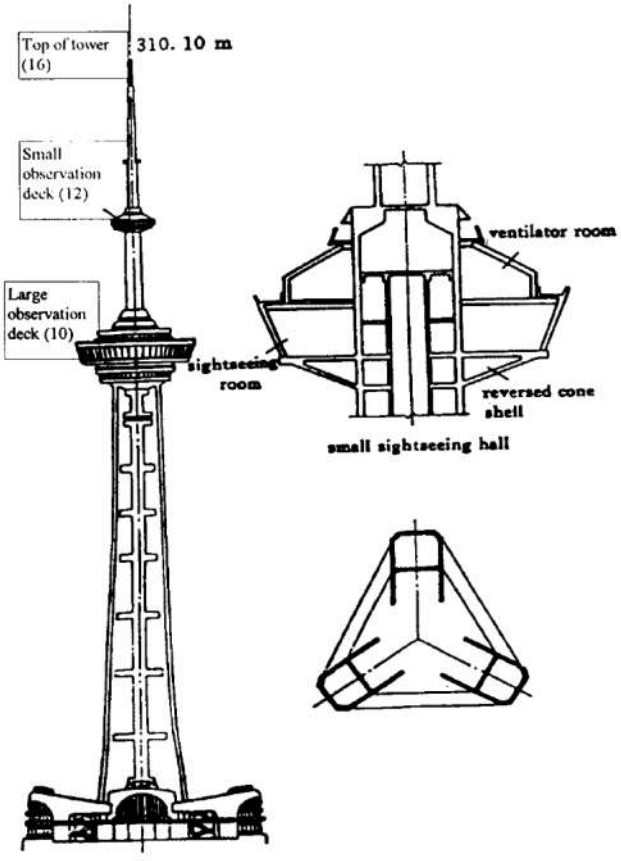

Figure 1 Nanjing TV tower (numbers in parentheses indicate nodes in model)

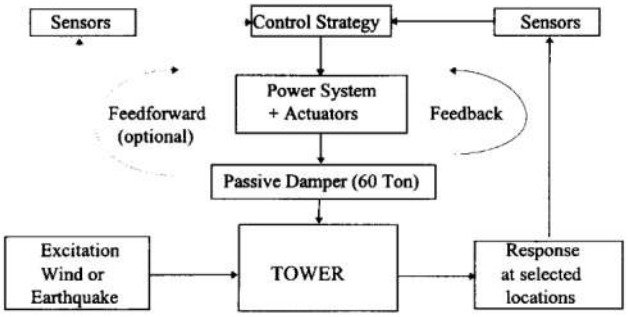

Figure 2 Block diagram of active control of tower

matic shown in *Figure 2*. The control strategy was developed using the modal approach as presented below.

3.1. Analytical model of controlled tower

Due to its symmetry, the tower can be idealized by a simple multidegree-of-freedom 'stick' model with masses lumped at critical locations. An extended 16 d.o.f. model was developed by Cheng *et al.*[11] using structural parameters. The damper is connected at the upper deck (d.o.f. 12) via suitable spring connections. The simplified diagram of the model is shown in *Figure 3*. The free body diagram of the mass damper (m_d) and the observation deck ($k = 12$) is shown in *Figure 3b*. The equations of motion in general terms for the tower and the AMD are:

$$\begin{cases} \mathbf{M}\ddot{\mathbf{X}}(t) + \mathbf{C}\dot{\mathbf{X}}(t) + \mathbf{K}\mathbf{X}(t) = \mathbf{F}_w(z,t) - \mathbf{D}f_d(t) \\ m_d\,(\ddot{x}_d + \ddot{x}_k) + f_d(t) = 0 \end{cases} \tag{1}$$

where **M**, **C** and **K** are mass, damping and stiffness matrices of the structure, $\mathbf{F}_w(t)$ is the wind force, and x_k and x_d are the displacement of the kth mass and the relative displacement of the mass damper m_d with respect to the kth mass ($k = 12$, for this case), respectively. The component d_j of the location vector **D** for the passive and active control force is:

$$d_j = \begin{cases} 0, & j \neq k \\ 1, & j = k \end{cases} \quad (k = 12 \text{ for this case}) \tag{2}$$

and the total force $f_d(t)$ exerted by the mass damper is

$$f_d(t) = c_d\dot{x}_d + k_d x_d + \epsilon m_d g\ \mathrm{sgn}[\dot{x}_d(t)] - u(t) \tag{3}$$

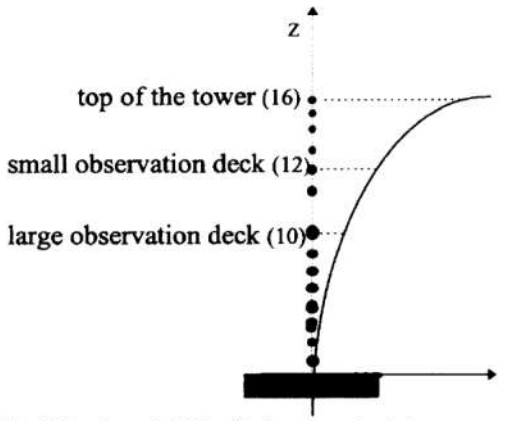

(a) Global modal (d.o.f's in parenthesis)

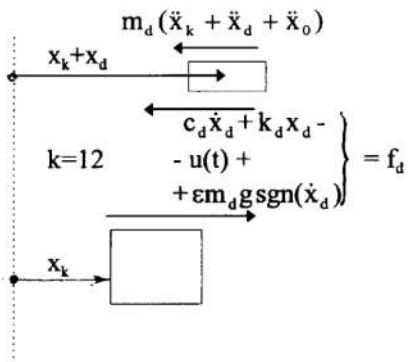

(b) Free body diagram at damper location (k).

Figure 3 Mathematical model of controlled tower

in which $u(t)$ is the force supplied by a hydraulic actuator upon command; ϵ is the friction coefficient between the mass damper and the kth floor.

The wind load can be expressed as[12]

$$\mathbf{F}_w(z,t) = v(t)\mathbf{S}(z) = v(t)s_k \tag{4}$$

where $v(t)$ is the dynamic wind speed at 10 m elevation, and parameter $\mathbf{S}(z)$ is the function of elevation z evaluated according to the procedure in the Appendix.

Assuming modal response:

$$\mathbf{X}(t) = \Phi Y(t) \tag{5}$$

in which Φ are the mode shapes of the uncontrolled tower, Φ_{kj} for $k = 12$ is equal unity ($\Phi_{12j} = 1$), the equations of motion, equation (1) can be transformed. Therefore, if $x_{12}(t) = \Sigma y_j(t)$:

$$\begin{cases} \ddot{y}_j + 2\xi_j\omega_j\dot{y}_j + \omega_j^2 y_j - \mu_j 2\xi_d\omega_d\dot{x}_d \\ \quad - \mu_j\omega_d^2 x_d = \Lambda_j v(t) - \dfrac{u^*(t)}{\hat{M}_j} \qquad j = 1, \ldots, m \\ \displaystyle\sum_{j=1}^{m} \ddot{y}_j + \ddot{x}_d + 2\xi_d\omega_d\dot{x}_d + \omega_d^2 x_d = +\frac{1}{m_d}\,u^*(t) \end{cases} \tag{6}$$

where

$$\Lambda_j = \frac{1}{\hat{M}_j}\sum_{i=1}^{n}\Phi_{ij}s_i,\ \mu_j = \frac{m_d}{\hat{M}_j},\ \hat{M}_j = \sum_{i=1}^{n}\Phi_{ij}^2 m, \tag{7}$$

$$u^* = u - \epsilon m_d g\ \mathrm{sgn}[\dot{x}_d(t)]$$

in which Λ_j are the jth mode participation factors for wind excitations, and u^* is described below.

Let us assume that x_{dj} and u_j are the 'modal' components of the mass damper movement (x_d) and the respective 'modal' correction force u, respectively. Although there is no apparent mathematical rigurosity in the assumption, the numerical evaluations indicate that for the sake of preliminary approximations this simplification is sufficiently accurate[12].

The first set in equation (6) shows modal independent equations. However, the last equation is coupled to each of the first through the summation term. For wind applications, the movement of the damper and active force can be assumed to have also modal components:

$$x_d = \sum_{j=1}^{m} x_{d_j},\ u^*(t) = \sum_{j=1}^{m} u_j^*(t) \tag{8}$$

which lead to independent equations for each mode, $i = j$

$$\ddot{y}_j + \ddot{x}_{d_j} + 2\xi_d\omega_d\dot{x}_{d_j} + \omega_d^2 x_{d_j} = \frac{1}{m_d}\, u_j^*(t). \tag{9}$$

The approximation introduced in such decoupling is discussed elsewhere[12]. Therefore, using such approximation, each mode can be analyzed independently using the state equation:

$$\dot{\mathbf{Z}}_j(t) = \mathbf{A}_j\mathbf{Z}_j(t) + \mathbf{B}_j u_j^*(t) + \mathbf{F}_j(t) \tag{10}$$

where

$$\mathbf{Z}_j(t) = \begin{bmatrix} y_j \\ x_{dj} \\ \dot{y}_j \\ \dot{x}_{dj} \end{bmatrix},$$

$$\mathbf{A}_j = \begin{bmatrix} 0 & 0 & 1 & 0 \\ 0 & 0 & 1 & 0 \\ -2\xi_j\omega_j & 2\mu_j\xi_{dj}\omega_{dj} & -\omega_j^2 & \mu_j\omega_{dj}^2 \\ 2\xi_j\omega_j & -2(1+\mu_j)\xi_{dj}\omega_{dj} & \omega_j^2 & -(1+\mu_j)\omega_{dj}^2 \end{bmatrix}$$

$$\mathbf{B}_j = \begin{bmatrix} 0 \\ 0 \\ -\dfrac{1}{\hat{M}_j} \\ \dfrac{1}{m_{dj}} + \dfrac{1}{\hat{M}_j} \end{bmatrix},\quad \mathbf{F}_j(t) = \begin{bmatrix} 0 \\ 0 \\ \Lambda_j \\ -\Lambda_j \end{bmatrix} v(t). \tag{11}$$

Solving the above equations for each mode, the approximated response can be obtained by modal superposition:

$$x_{max} = \sqrt{\sum_{j=1}^{m} x_{jmax}^2}\ . \tag{12}$$

3.2. *Control laws*

The mass damper can be activated as a passive device or can be controlled by an external control algorithm (see *Figure 2*). Several control laws for active alternatives were verified and evaluated during the design process. These control laws include linear and nonlinear strategies:

(a) linear quadratic regulator (LQR) algorithms;
(b) nonlinear feedback control algorithms.

The algorithms used for evaluation are listed below with a brief description of their main parameters. These algorithms have been studied previously by others[13].

3.2.1. *LQR algorithms*

(a) Complete (implicit) algorithm. The control force $u_j(t)$ is obtained from feedback of state variables and accelerations:

$$u_j(t) = -G_jZ_j(t) = -[g_1^*\ g_2^*\ g_3^*\ g_4^*\ g_5^*\ g_6^*]\ [y_j\ x_{dj}\ \dot{y}_j\ \dot{x}_{dj}\ \ddot{y}_j\ \ddot{x}_{dj}]^T \tag{13}$$

in which control gain g_j^* can be expressed by the normalized control gain g_j

$$[g_1^*\ g_2^*\ g_3^*\ g_4^*\ g_5^*\ g_6^*] = m_d\left[\frac{g_1}{\mu}\,\omega_1^2\ g_2\omega_d^2\ 2\,\frac{g_3}{\mu}\,\xi_1\omega_1\ 2g_4\xi_d\omega_d\ \frac{g_5}{\mu}\ g_6\right]. \tag{14}$$

The control matrix G_j can be obtained by an optimal search for minimal modal response suggested by the first author[12].

(b) *State feedback.* The control force u_j can be calculated using the well known state feedback approach which includes only the state variables in equation (14) (without the accelerations), i.e. $g_5^* = g_6^* = 0$. The rest of the gain coefficients are obtained from:

$$\mathbf{G}_j = -\mathbf{R}^{-1}\mathbf{B}_j\mathbf{P} \tag{15}$$

where matrix $\mathbf{P}$ is the solution of the Riccati equation[4]

$$\mathbf{P}\mathbf{A}_j + \mathbf{A}_j^T\mathbf{P} - \mathbf{P}\mathbf{B}_j\mathbf{R}^{-1}\mathbf{B}_j^T\mathbf{P} + \mathbf{Q} = 0. \tag{16}$$

It should be noted that the selection of the weight matrices $\mathbf{Q}$ and R is critical for the LQR control and a search for an optimum configuration was performed in the design process.

(c) *State velocity feedback.* State velocity feedback includes only the 'velocity' of the state variables, that is $g_1^* = g_2^* = 0$. The rest of the coefficients are obtained from[13]:

$$u_j(t) = -\mathbf{G}_{1_j}\dot{\mathbf{Z}}_j(t) = -[\mathbf{I} - \mathbf{G}_j\mathbf{A}_j^{-1}\mathbf{B}_j]^{-1}\ \mathbf{G}_j\mathbf{A}_j^{-1}\mathbf{Z}_j(t) \tag{17}$$

where G_j is obtained from equation (16). The advantage of this formulation stems from the direct use of non-reference sensors such as velocity transducers and accelerometers.

3.2.2. Nonlinear feedback control algorithms Recently, nonlinear control algorithms were shown to reduce substantially extreme peaks[13]. The simplest form of an efficient nonlinear algorithm is a polynomial of control variables including odd power only. Using a first-order (cubic) polynomial the control gains in equation (14) are obtained as[13]:

$$\begin{aligned}\mathbf{G} = [&g_1^*\{1 + \alpha_1 y_1^2(t)\}\ g_2^*\{1 + \alpha_2\dot{x}_d^2(t)\} \\ &g_3^*\{1 + \alpha_3\dot{y}_1^2(t)\}\ g_4^*\{1 + \alpha_4\dot{x}_d^2(t)\} \\ &g_5^*\{1 + \alpha_5\dot{y}_1^2(t)\}\ g_6^*\{1 + \alpha_6\dot{x}_d^2(t)\}]\end{aligned} \tag{18}$$

for the complete feedback. For the state and state velocity feedback, $g_5^* = g_6^* = 0$ and $g_1^* = g_2^* = 0$, respectively. The gain factors are obtained for selected parameters α_i using the solution of the Ricatti equation[13]. Although this method produces better corrections of peak responses, for this application, the linear algorithms, state feedback and velocity feedback were selected for further evaluation and implementation.

4. Performance of the tower with mass damper

The mass damper that can produce the necessary reductions to limit the response near the comfort limits was first

Table 1 Load specifications

	Structural parameters										Wind parameters*				
	elevation	length	width	mass	mode shapes					$D(z)$				
	z_i	h_i	b_i	m_i				μ_s	μ_z	$= h_i^* b_i$	$s(z)$	Λ_{1i}	Λ_{2i}	Λ_{3i}
nod	(m)	(m)	(m)	(t)	1st	2nd	3rd	(—)	(—)	(m^2)	(KNs/m)	(m/s^2)	(m/s^2)	(m/s^2)
(1)	(2)	(3)	(4)	(5)	(6)	(7)	(8)	(9)	(10)	(11)	(12)	(13)	(14)	(15)
16	310.1	11.0	0.750	4	1.873	8.333	−22.376	1.30	3.00	4.13	0.416	0.00014	0.0070	−0.00171
15	299.1	13.0	1.100	12	1.704	6.330	−11.327	1.30	2.97	11.28	1.125	0.00034	0.00140	−0.00234
14	286.1	16.0	1.800	18.7	1.521	4.467	−3.366	1.30	2.92	21.55	2.120	0.00057	0.00186	−0.00131
13	270.1	29.7	3.500	165.1	1.325	2.935	−0.137	1.30	2.87	66.38	6.411	0.00150	0.00369	−0.00016
12	**240.4**	**41.2**	**6.000**	**1253.9**	**1.000**	**1.000**	**1.000**	**1.20**	**2.77**	**175.58**	**15.081**	**0.00267**	**0.00296**	**0.00277**
11	199.2	13.4	13.420	1512.4	0.652	−0.264	0.043	1.20	2.60	213.51	17.269	0.00199	−0.00089	0.00014
10	185.8	14.0	13.420	2678.6	0.576	−0.290	−0.053	1.20	2.55	183.85	14.542	0.00148	−0.00083	−0.00014
9	171.8	13.2	13.420	3395.3	0.500	−0.296	−0.127	1.20	2.48	182.51	14.079	0.00125	−0.00082	−0.00033
8	158.6	20.8	13.950	1322.3	0.431	−0.288	−0.177	1.39	2.42	233.65	20.391	0.00155	−0.00115	−0.00066
7	137.8	18.0	14.700	1628.1	0.330	−0.258	−0.218	1.39	2.32	277.38	23.143	0.00135	−0.00117	−0.00093
6	119.8	18.0	15.450	1624.5	0.253	−0.219	−0.220	1.39	2.21	271.35	21.648	0.00097	−0.00093	−0.00087
5	101.8	21.6	17.100	1917.9	0.186	−0.175	−0.198	1.39	2.10	323.73	24.515	0.00081	−0.00084	−0.00089
4	80.2	21.6	18.750	2319.8	0.120	−0.122	−0.152	1.39	1.95	387.18	27.166	0.00058	−0.00065	−0.00076
3	58.6	26.4	20.228	2820.1	0.068	−0.073	−0.099	1.39	1.76	469.50	29.795	0.00036	−0.00043	−0.00054
2	32.2	22.1	24.345	3186.7	0.024	−0.028	−0.041	1.39	1.45	536.02	28.084	0.00012	−0.00015	−0.00021
1	10.1	10.1	28.560	3992.9	0.005	−0.006	−0.010	1.39	1.00	413.24	14.940	0.00001	−0.00002	−0.00003
0	0.0		modal mass $\hat{M}_i$		**5653**	5095	5444		participation factor Λ_i			0.01569	0.00270	−0.00798

*Notations see in Appendix A.

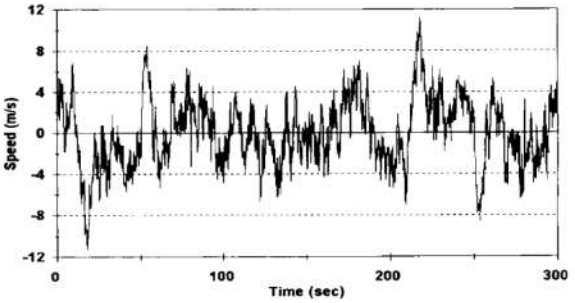

Figure 4 Simulated wind speed (Davenport spectrum)

designed globally, i.e. the size of the mass and the necessary spring and damping ratios were established using simplified formulations assuming first mode response only with a mass ratio of $\mu \approx 1.0\%$. This results in a mass of 60 tons ($\approx$130 Kips). The optimal damping ratio for a mass damper tuned to the first mode frequency of the tower is $\xi_{opt} \approx 7\%$. The response of the tower structure without and with the mass damper was first evaluated for the wind and earthquake action. The dynamic parameters of the tower used in the analysis and the wind parameters are shown in *Table 1*. The wind history was obtained from Davenport spectrum[14] adjusted for the wind code of China (see Appendix). A sample realization of the wind speed history, $v(t)$, is shown in *Figure 4*.

The response of structure without and with the mass damper are shown in *Figure 5*. The response of the observation deck with a passive tuned mass damper (TMD), without an external active force (see *Figure 6*), has reduced values compared to the response of the tower alone. However, the response is far beyond the target comfort limit of 15 mg. The sample response of the tower using the mass damper with active control (AMD) based on state and state velocity feedback mentioned above is shown in *Table 2*. The response obtained is near the comfort limit of 15 mg with the active damper, following a reduction of more than 40% in acceleration and more than 30% in displacement, given the space, force and power constraints, as explained in the next section. The acceleration of the observation deck and the mass stroke of the AMD are shown in *Figures 6* and *7*.

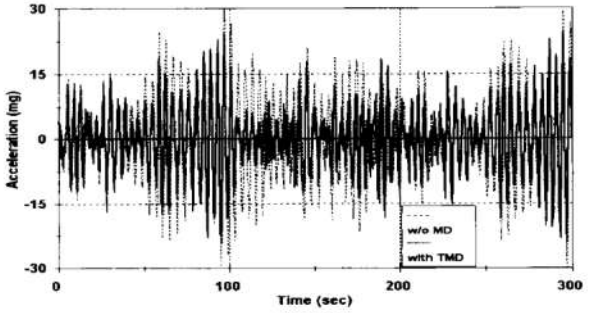

Figure 5 Acceleration at the observation deck with TMD

The tower was analyzed and evaluated for several alternatives of mass damper design. Alternative, passive dampers, each tuned to one of the first three modes, and alternative dampers with active control, were evaluated. The modal response obtained by the approximation explained in the previous section is shown in *Table 3*. The overall response is mostly affected by the first mode. The response tuned to the first mode, either passive or active, is reduced substantially [see case (b) and (e) in *Table 3*]. The total response is influenced by the higher modes by only 10–15%. The alternative tuning to higher modes cannot control the total tower movement. However, the reduction in the

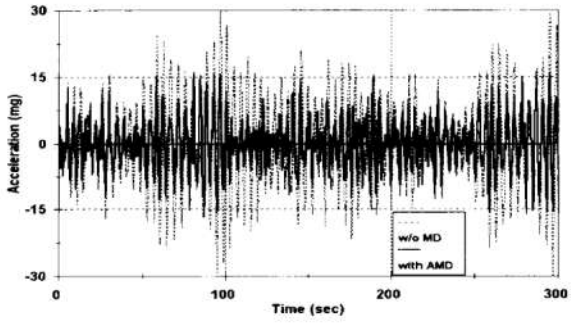

Figure 6 Acceleration at the observation deck with AMD (state velocity feedback)

Table 2 Response of observation deck and mass damper ($\xi_1 = 0.02$ $m_d = 60$ tons, $\xi_d = 0.07$, mass stroke = ± 0.75 m)

Control gains						Displacements			Velocities			Accelerations			Control resources		
						damper	deck	reduction*	damper	deck	reduction*	damper	deck	reduction*	force	flow	flow
g_1	g_2	g_3	g_4	g_5	g_6	x_d (m)	x_{12} (m)	(%)	$\dot{x}_d$ (m/sec)	$\dot{x}_{12}$ (m/sec)	(%)	$\ddot{x}_d$ (mg)	$\ddot{x}_{12}$ (mg)	(mg)	F_d (kN)	Q_{max} (gpm)	Q_{avg} (gpm)
(1)	(2)	(3)	(4)	(5)	(6)	(7)	(8)	(9)	(10)	(11)	(12)	(13)	(14)	(15)	(16)	(17)	(18)
(a) Uncontrolled (UC)																	
0.000	0.000	0.000	0.000	0.000	0.000	0.000	0.137	—	0.000	0.185	—	0.0	31.8	—	—	—	—
(b) Tuned mass damper (TMD)																	
0.000	0.000	0.000	0.000	0.000	0.000	0.512	0.104	24.4	0.767	0.138	25.6	121.8	24.3	23.7	—	—	—
(c) Active mass damper (AMD) — State feedback																	
−0.551	8.609	25.384	36.658	0.000	0.000	0.750	0.091	33.7	1.061	0.096	48.3	303.7	17.8	43.9	208.1	94.7	10.6
(c) Active mass damper (AMD) — State velocity feedback																	
0.000	0.000	1.976	9.574	0.174	−0.360	0.750	0.089	35.1	1.326	0.095	48.8	316.8	16.0	49.6	152.7	86.2	11.3

*Reduction relative to uncontrolled (UC).

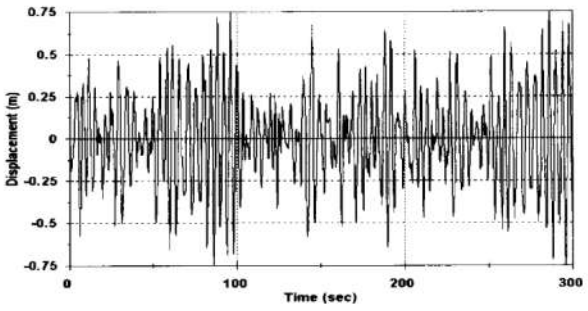

Figure 7 Displacement of AMD x_d (state velocity feedback)

first mode response and the reduction in the total response are almost the same. Therefore, the design using exclusively the first mode as a preliminary performance evaluator is representative to the multi-modal approach. This is characteristic to cantilever towers, either in wind storms or earthquakes. For each alternative, the individual modal response for which the damper was tuned, is strongly affected by the dampers. However, inspecting the overall response, the contribution of the first mode is predominant.

5. Design of damper in the presence of constraints

The TV tower to be controlled is an existing structure, as specified above. The space available for the implementation of a damper is limited to an elevated surface in the upper observation deck bound by existing walls. The support structure has limited strength and the power necessary is limited by access space, construction limits and existing power supplies. Therefore, the design of the mass damper was developed with following restrictions:

(a) *Space restrictions.* The space available for the damper is a surface shaped as a ring with a 2.5 m radial width. The damper had to be elevated from the floor to allow use of floor space for storage. The mass, therefore, was designed as a closed ring with an internal radius of 3.9 m and an external radius of 4.75 m (see *Figure 8*). This design allows for the movement of the damper of ± 750 mm. This limit was considered in the simulations shown in the previous sections. Additional simulations indicated that, given more space the tower response can be reduced substantially more. The physical stroke is limited by shock absorbers (springs) mounted against the central core wall.

Table 3 Modal response with mass damper

	Displacement		Velocity		Acceleration		
	damper	deck	damper	deck	damper	deck	Control force
	x_d	x_{12}	$\dot{x}_d$	$\dot{x}_{12}$	$\ddot{x}_d$	$\ddot{x}_{12}$	F_d
mode	(m)	(m)	(m/s)	(m/s)	(mg)	(mg)	(kn)
(1)	(2)	(3)	(4)	(5)	(6)	(7)	(8)
				(a) Uncontrolled			
1	0.000	0.135	0.000	0.181	0.000	30.1	0.000
2	0.000	0.004	0.000	0.013	0.000	5.3	0.000
3	0.000	0.002	0.000	0.013	0.000	10.8	0.000
srss	0.000	0.135	0.000	0.182	0.000	33.2	0.000
				(b) with TMD tuned to the 1st mode (passive control)			
1	0.509	0.104	0.794	0.138	125.2	24.0	0.000
2	0.005	0.004	0.017	0.013	6.4	5.3	0.000
3	0.003	0.002	0.015	0.013	11.2	10.7	0.000
srss	0.510	0.104	0.795	0.139	125.9	26.8	0.000
				(c) with TMD tuned to the 2nd mode (passive control)			
1	0.022	0.143	0.059	0.193	19.6	32.4	0.000
2	0.011	0.003	0.044	0.009	17.8	3.6	0.000
3	0.003	0.002	0.021	0.013	14.5	10.5	0.000
srss	0.025	0.143	0.076	0.193	30.2	34.3	0.000
				(d) with TMD tuned to the 3rd mode (passive control)			
1	0.005	0.142	0.018	0.192	9.5	32.3	0.000
2	0.001	0.004	0.006	0.013	3.0	5.2	0.000
3	0.005	0.002	0.040	0.009	32.5	6.3	0.000
srss	0.007	0.142	0.044	0.193	34.0	33.3	0.000
				(e) with ATMD tuned to the 1st mode (active control)			
1	0.722	0.088	1.248	0.089	262.7	17.4	102.6
2	0.033	0.002	0.135	0.006	69.5	2.5	36.1
3	0.037	0.002	0.276	0.010	269.9	9.7	151.6
srss	0.723	0.088	1.286	0.090	383.0	20.1	186.6
				(f) with ATMD tuned to the 2nd mode (active control)			
1	0.275	0.120	0.469	0.160	162.1	26.9	232.3
2	0.021	0.002	0.080	0.007	34.7	3.0	16.2
3	0.019	0.002	0.130	0.005	109.1	4.6	47.8
srss	0.277	0.120	0.494	0.160	198.5	27.5	237.7
				(g) with ATMD tuned tothe 3rd mode (active control)			
1	0.088	0.138	0.150	0.187	162.1	31.4	297.9
2	0.010	0.003	0.040	0.0.0	28.0	3.8	27.6
3	0.010	0.002	0.074	0.006	82.7	4.8	47.8
srss	0.089	0.138	0.172	0.187	184.2	32.0	303.0

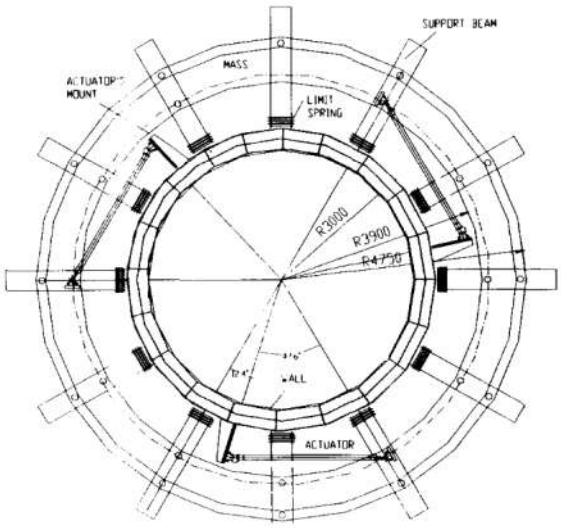

Figure 8 Plan of AMD system

(b) *Weight restrictions*. The weight of the damper was limited by the support structure to 60 tons. The mass will be made of lead bricks which are higher weight density than other metals and also allow on site easy construction. A heavier damper would affect the response more, as shown by numerical studies.

(c) *The support structure*. The support system for the mass includes 12 frames as shown in *Figure 9*. Those frames are supported on the beams of the existing floor of the observation deck and on the core wall of the tower. The frame provides support for the mass ring through a Teflon–steel interface.

(d) *Spring construction*. The mass was designed to slide on the low friction Teflon–steel interface. The restoring spring for the construction of the damper require a large stroke and low stiffness. An evaluation of nitrogen (gas) springs devices and of mechanical springs, shows substantial limitations and high costs. At the same time the size of the spring force and of the total active control force proved to be of the same order of magnitude and somewhat out-of-phase. Therefore, it was decided to produce the

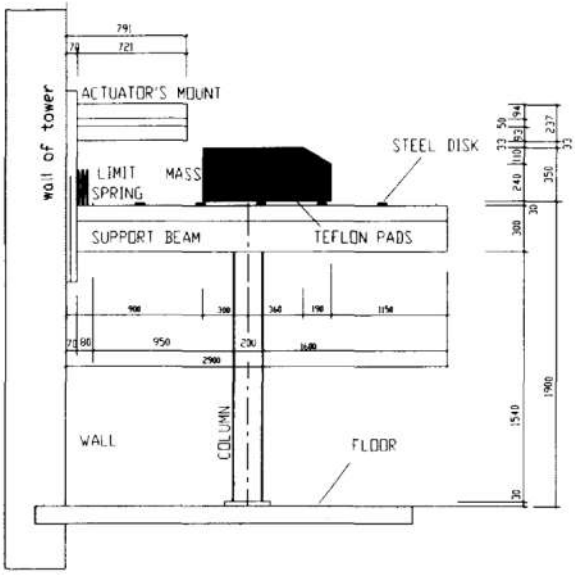

Figure 9 Details of cross-section of supporting frame

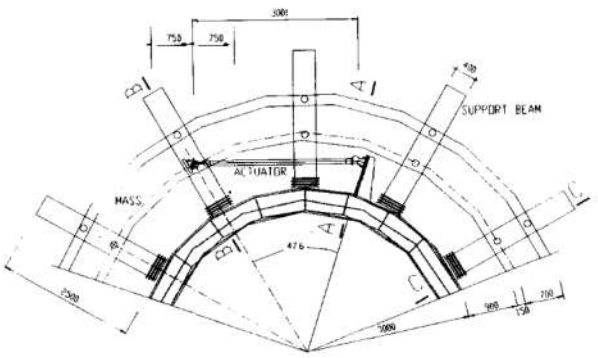

Figure 10 Details of actuator connection

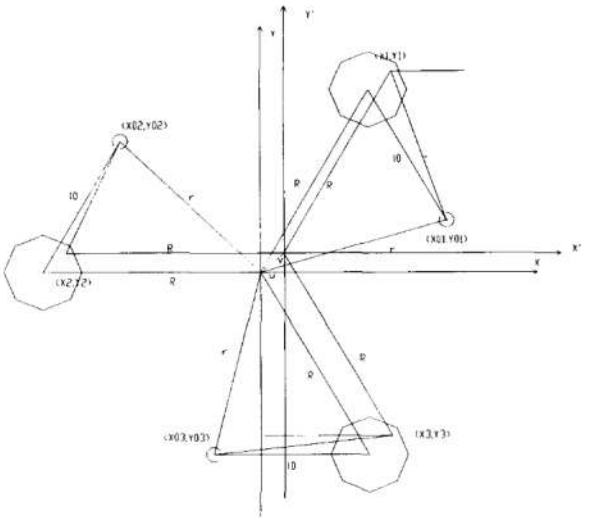

Figure 11 Displacement of actuators

restoring force ($k_d x_d$) through the active actuators as part of the total control force f_d (from equation (3)):

$$f_d(t) = c_d\dot{x}_d + k_d x_d + \epsilon m_d g \operatorname{sgn}\dot{x}_d - u(t). \tag{19}$$

(e) *The actuators*. The actuators with a stroke of 1.50 m and a total length of 4.5 m were selected such that will integrate in the circular design of mass damper and make best use of the space available (see *Figures 8* and *10*). Three, 100 kN, hydraulic actuators arranged at 120° to each other were found suitable to supply the necessary forces.

(f) *Power*. The hydraulic power is provided by pumps which can supply the required peak flows. The alternative of use of accumulators and a smaller power supply was found to be more expensive for a wind application, which may require long time sustained operation at peak requirements.

(g) *Rotational coupling* of actuators produces a resultant force, which may torque the mass. The design of the damper requires to produce lateral corrections only, therefore, the torque had to be eliminated using a rigid transformation (see *Figure 11*):

$$\mathbf{F} = \begin{bmatrix} F_1 \\ F_2 \\ F_3 \end{bmatrix} = \tag{20}$$

$$\begin{bmatrix} \cos\theta_1 & \cos\theta_2 & -\cos\theta_3 \\ \sin\theta_1 & \sin\theta_2 & -\sin\theta_3 \\ \cos(\theta_1+30) & \sin\theta_2 & \cos(\theta_3-30) \end{bmatrix}^{-1} \begin{bmatrix} F_x \\ F_y \\ 0 \end{bmatrix}$$

where F_x and F_y are the active forces needed in x- and y-axes, and θ_i are function of displacement of the mass center x_d and y_d

$$\theta_i = \tan^{-1} \frac{l_0 \sin\theta_{i0} + y_d}{l_0 \cos\theta_{i0} + x_d}, \quad \theta_{10} = -60,\ \theta_{20} = 60,\ \theta_{30} = 0. \tag{21}$$

It should be noted that the transformation matrix should be updated during the control implementation through the measurement of displacements x_d and y_d. This results in a nonlinear control strategy, which was also considered in the design.

(h) *Effect of friction* in the supporting of Teflon pads is of extreme importance. The formulations in the previous sections include the friction effect. The real control force to overcome the frictional effect should include, therefore, the friction as shown in equation (19). The effect of friction force on the controlled tower is summarized in *Table 4*. While the response with the tuned mass damper (TMD) deteriorates with the increasing friction coefficients such that it cannot be used, the response with the AMD can be controlled by adjusting the control gains (see *Table 4*). This, however, requires an increase of control force demand and the power requirements. The design selected for this application has a friction coefficient of 4%, characteristic to high pressure Teflon–steel interfaces.

6. Remarks and conclusions

The design of the active mass damper was implicitly influenced by the performance targets (in this case guided by service comfort), by the selection of control strategy and by the physical constraints imposed by the implementation. None of the above could be independently considered in the design of the mass damper. The design of a larger mass damper, using larger control forces can produce substantial reductions of the response of the tower. However, given the space and strength constraints, the active system can produce a better response than the passive system. Moreover, using non-reference sensors such as linear velocity feedback or a nonlinear control strategy, the response reductions can be maximized with the same resources. The other implementational problems related to time delay and force nonlinearities can be solved through the detailed design of control gains with suitable compensation.

Table 4 Comparison of controlled response in presence of friction of mass damper

	friction ratio	displacement			velocity			acceleration			control resources		
		damper	deck	reduction	damper	deck	reduction	damper	deck	reduction	force	flow	flow
	ϵ	x_d	x_{12}		$\dot{x}_d$	$\dot{x}_{12}$		$\ddot{x}_d$	$\ddot{x}_{12}$		F_d	Q_{max}	Q_{avg}
case	(%)	(m)	(m)	(%)	(m/s)	(m/s)	(%)	(mg)	(mg)	(%)	(kn)	(gpm)	(gpm)
(1)	(2)	(3)	(4)	(5)	(6)	(7)	(8)	(9)	(10)	(11)	(12)	(13)	(14)
						(a) Uncontrolled							
		0	0.137	0	0	0.185	0.0	0.0	31.8	0.0	—	—	—
						(b) TMD							
1	0	0.512	0.104	24.4	0.767	0.138	25.6	121.8	24.3	23.6	—	—	—
2	0.5	0.381	0.115	16.69	0.593	0.154	17	97.4	26.5	16.5	—	—	—
3	1.0	0.272	0.128	6.7	0.426	0.172	7.0	75.4	29.6	6.9	—	—	—
4	1.5	0.165	0.139	−1.2	0.278	0.187	−1.1	54.4	32.1	−1.1	—	—	—
5	2.0	0.067	0.144	−4.5	0.195	0.194	−4.4	36.4	33.2	−4.4	—	—	—
6	3.0	0.011	0.145	−5.2	0.207	0.194	−4.9	32.2	33.3	−4.8	—	—	—
						(c) AMD (considering friction effect in active control force)							
1	0.0	0.761	0.089	35.5	1.252	0.094	49.5	308.8	15.8	50.4	153.3	85.2	11.4
2	1.0	0.759	0.089	35.6	1.254	0.093	49.6	308.7	15.8	50.4	154.4	86.5	11.4
3	1.5	0.758	0.088	35.6	1.256	0.093	49.7	308.7	15.8	503	156.3	87.8	11.5
4	2.0	0.757	0.088	35.6	1.26	0.093	49.7	308.6	15.8	50.2	158.3	89.2	11.6
5	3.0	0.755	0.088	35.6	1.267	0.093	49.8	308.6	15.8	50.1	166.8	92.0	11.9
6	4.0	0.753	0.088	35.7	1.272	0.093	50.0	308.4	15.9	50.0	170.2	94.8	12.4
7	5.0	0.753	0.088	35.7	1.283	0.092	50.4	308.3	15.9	49.9	175.3	97.5	13.0
8	8.0	0.756	0.089	35.4	1.379	0.092	50.5	307.2	16.2	48.9	187.1	109.2	15.6
9	10.0	0.755	0.089	35.2	1.312	0.089	51.9	311.2	16.1	49.5	202.8	118.4	17.9
10	15.0	0.791	0.092	33.3	1.463	0.095	49.0	356.3	18.1	42.9	226.3	160.0	24.7
11	20.0	0.838	0.089	35.1	1.659	0.103	44.4	416.3	19.6	38.3	256.9	198.6	31.5
12	0.0	0.762	0.089	35.5	1.251	0.094	49.4	308.8	15.7	50.5	150.6	83.8	11.4
						(d) AMD (without considering friction effect in active control force)							
1	0.5	0.755	0.089	35.1	0.230	0.094	49.2	311.6	16.0	49.6	149.5	84.0	11.0
2	1.0	0.747	0.090	34.6	0.213	0.095	49.0	314.3	16.3	48.8	148.4	84.0	10.6
3	1.5	0.743	0.090	34.1	1.197	0.095	48.6	317.0	16.6	47.9	146.7	84.0	10.3
4	2.0	0.740	0.091	33.7	1.187	0.096	48.4	319.6	16.8	47.0	154.7	83.7	10.0
5	3.0	0.735	0.092	32.7	1.178	0.097	47.6	325.0	17.4	45.3	155.4	87.3	9.5
6	4.0	0.729	0.094	31.8	1.171	0.098	47.0	330.1	17.9	43.6	153.8	92.1	9.2
7	5.0	0.722	0.095	30.8	1.167	0.100	46.0	335.0	18.4	41.9	152.8	96.2	9.1
8	8.0	0.703	0100	27.1	1.179	0.108	41.5	350.0	20.0	36.9	147.6	109.3	9.3
9	10.0	0.679	0.103	25.3	1.240	0.114	38.7	348.7	21.2	33.3	175.7	111.3	9.4
10	15.0	0.628	0.108	21.1	1.290	0.126	32.0	376.1	23.9	24.8	181.3	129.9	10.1
11	20.0	0.584	0.113	17.9	1.203	0.134	27.6	386.5	24.8	22.0	210.2	144.0	10.4

Note: control gains used in ATMD are: $g_3 = 1.140$, $g_4 = 0.831$, $g_5 = 0.205$, $g_6 = -0.165$.

Acknowledgements

This work is supported by a grant from the National Science Foundation enrolled in a US–People's Republic of China cooperation program, grant number CMS-9402196. The support is greatly acknowledged. The authors are grateful to the advice and contribution of Professors J. N. Yang and Maria Feng of University of California at Irvine, Professor Shinozuka of University of Southern California and of Mr A. Clark and N. Peterson of MTS Corporation of Minneapolis, Minnesota.

Appendix

An introduction to 'wind load standard code of China'

The dynamic wind load subjected to the structure is

$$f_w(z,t) = \mu_s D(z) w(z,t) \tag{A1}$$

in which $D(z)$ is the windface area and μ_s is drag coefficient (i.e. $\mu_s = 1.2$ for circular sections, $\mu_s = 1.3$ for rectangular sections, $\mu_s = 1.2$ for triangular sections); $w(z,t)$ is dynamic wind pressure at elevation z:

$$w(z,t) = \mu_z w_0(t) = [(0.1z)^{2\alpha}][\rho \bar{v}_{10} v(t)] \tag{A2}$$

where μ_z is the wind profile coefficient and $w_0(t)$ is the reference wind pressure (usually at 10 m elevation), respectively: i.e. $\mu_z = (0.1z)^{2\alpha}$ and $w_0(t) = \rho \bar{v}_{10} v(t)$, where α is the roughness coefficient (in the present case $\alpha = 0.16$) and ρ is the air density (≈ 0.00125 kg/m^3); $\bar{v}_{10} = 20.7$ m/s and $v(t)$ are the mean wind speed and the dynamic wind speed at 10 m elevation, respectively. Therefore, if a function $s(z)$ is defined as:

$$s(z) = 0.00125 \mu_s \mu_z D(z) \bar{v}_{10} \tag{A3}$$

then the wind force can be expressed as (see equation (4) in this paper):

$$f_w(z,t) = s(z) v(t). \tag{A4}$$

References

1 Higashino, M., Aizawa, S. and Kobayashi, K. 'The study of torsional-translational control by the active mass damper of practical use', *Proc. Jpn Nat. Symp. Workshop on Struct. Response Control*, 1992, pp 203–208

2 Soong, T. T., Reinhorn, A. M., Aizawa, S. and Higashino, M. 'Recent structural applications of active control technology', *J. Struct. Control* 1994, **1** (2), 15–21

3 Kobori, T. 'Future direction on research and development of seismic-response-controlled structure', *Proc. 1st World Conf. Struct. Control*, Pasadena, CA, 1994, Panel-19-31

4 Soong, T. T. *Active structural control: theory and practice*, Longman and Wiley, London, New York, 1990

5 Soong, T. T., Reinhorn, A. M., Wang, Y. P. and Lin, R. C. 'Full scale implementation of active control, Part I: System design and simulation results', *ASCE/J. Struct. Engng* 1991, **117** (11), 3516–3536

6 Reinhorn, A. M., Soong, T. T., Riley, M. A., Lin, R. C., Aizawa, S. and Higashiho, M. 'Full scale implementation of active control, part II: installation and performance', *ASCE/J. Struct. Engng* 1993, **119** (11), 2317–2332

7 Fukuyama, K., Mine, T., Masuda, Y., *et al.* 'Active mass damper using the weight of rooftop heliport', *Dynamic and Design Conf. - 93*, Movic, Japan, 1993, pp 156–160

8 Fujita, T. 'Hybrid mass dampers with convertible active and passive modes for vibration control of tall buildings', *Proc. Int. Workshop on Struct. Control*, Honolulu, Hawaii, 1993, pp 151–165

9 Grossman, J. S. 'Slender concrete structures – the new edge', *ACI Struct. J.* 1990, **87** (1), 39–52

10 Peterson, N. 'Design of large scale tuned mass damper', in *Structural control*, Leipholz, H. H. E. (eds), North-Holland, Amsterdam, 1980, pp 581–596

11 Cheng, W., Qu, W. and Li, A. 'Hybrid vibration control of Nanjing TV tower under wind excitation', *Proc. 1st World Conf. Structural Control*, Pasadena, CA, Vol. 1, 1994, pp 32–34

12 Cao, H. 'Guidelines for design of active tuned mass dampers', Ph.D. dissertation, State University of New York at Buffalo, 1997

13 Wu, Z. G. 'Nonlinear feedback strategies in active structural control', Ph.D. dissertation, State University of New York, Buffalo, 1995

14 Simiu, E. and Scanlan, R. H. *Wind effects on structures* (2nd edn), Wiley, New York, 1986, p 64